




## ORIGINAL ARTICLE

# Deep immune profiling of patients with renal impairment unveils distinct immunotypes associated with disease severity

I-Wen Wu<sup>1,2</sup>, Yi-Lun Wu<sup>3</sup>, Huang-Yu Yang<sup>2,4,5</sup>, Cheng-Kai Hsu <sup>1</sup>, Lun-Ching Chang <sup>6</sup>, Yuh-Ching Twu <sup>7</sup>, Ya-Ling Chang<sup>8</sup>, Wen-Hung Chung<sup>9</sup>, Chih-Wei Yang<sup>2,4</sup>, Wen-Ping Hsieh<sup>3</sup> and Shih-Chi Su<sup>9</sup>

<sup>1</sup>Department of Nephrology, Chang Gung Memorial Hospital, Keelung, Taiwan, <sup>2</sup>College of Medicine, Chang Gung University, Taoyuan, Taiwan, <sup>3</sup>Institute of Statistics, National Tsing-Hua University, Hsinchu, Taiwan, <sup>4</sup>Kidney Research Center, Department of Nephrology, Chang Gung Memorial Hospital, Linkuo, Taiwan, <sup>5</sup>Department of Health Policy and Management, Johns Hopkins Bloomberg School of Public Health, Baltimore, MD, USA, <sup>6</sup>Department of Mathematical Sciences, Florida Atlantic University, Boca Raton, FL, USA, <sup>7</sup>Department of Biotechnology and Laboratory Science in Medicine, National Yang Ming Chiao Tung University, Taipei, Taiwan, <sup>8</sup>Advanced Immunology Laboratory, Chang Gung Memorial Hospital, Linkuo, Taiwan and <sup>9</sup>Whole-Genome Research Core Laboratory of Human Diseases, Chang Gung Memorial Hospital, Keelung, Taiwan

Correspondence to: Shih-Chi Su; E-mail: [ssu1@cgmh.org.tw](mailto:ssu1@cgmh.org.tw)

## ABSTRACT

**Background.** Chronic kidney disease (CKD) is pathologically correlated with a sophisticated milieu of innate and adaptive immune dysregulation, but the underlying immunological disturbances remain poorly understood.

**Methods.** To address this, we comprehensively interrogated cellular and soluble elements of the immune system by using high-dimensional flow cytometry to analyze peripheral blood mononuclear cells and performing cytokine/chemokine profiling of serum samples, respectively, in a cohort of 69 patients and 19 non-CKD controls.

**Results.** Altered serum levels of several cytokines/chemokines were identified, among which concentrations of stem cell factor (SCF) were found to be elevated with the progression of CKD and inversely correlated with estimated glomerular filtration rate (eGFR). Deep immunophenotyping analyses reveal a global change in immune modulation associated with CKD severity. Specifically, a decrease in the subsets of CD56<sup>dim</sup> natural killer (NK) cells (KLRG-1<sup>+</sup>CD38<sup>+</sup>CD64<sup>+</sup>CD15<sup>+</sup>CD197<sup>+</sup>) and monocytes (KLRG-1<sup>+</sup>CD38<sup>+</sup>PD-1<sup>+</sup>) was detected in severe CKD compared with controls and mild CKD. In addition, comparisons between mild and severe CKD demonstrated a loss of a mature B cell population (PD-1<sup>+</sup>CD197<sup>+</sup>IgD<sup>+</sup>HLA-DR<sup>+</sup>) in the advanced stages of disease. Further, we identified immunophenotypic markers to discriminate mild CKD from the controls, among which the portion of CD38<sup>+</sup> monocytes was of particular value in early diagnosis.

**Conclusions.** Our data unveil severity-specific immunological signatures perturbed in CKD patients.

Received: 28.3.2022; Editorial decision: 30.7.2022

© The Author(s) 2022. Published by Oxford University Press on behalf of the ERA. This is an Open Access article distributed under the terms of the Creative Commons Attribution-NonCommercial License (<https://creativecommons.org/licenses/by-nc/4.0/>), which permits non-commercial re-use, distribution, and reproduction in any medium, provided the original work is properly cited. For commercial re-use, please contact [journals.permissions@oup.com](mailto:journals.permissions@oup.com)

## LAY SUMMARY

Prolonged uremic conditions cause a dynamic immune dysregulation. Yet, current studies of immune dysfunction in chronic kidney disease (CKD) have been mostly focused on a particular immune cell lineage and on the advanced stages of disease. Here, we present a comprehensive atlas of immune modulation associated with the progression of CKD by evaluating a panel of circulating cytokines/chemokines/growth factors and conducting high-dimensional measurements of peripheral blood mononuclear cells in CKD patients with different disease severities. Our data-driven approaches identified distinct subsets of monocytes, B cells and natural killer cells with specific activation status perturbed during renal impairment, which may have etiological and diagnostic implications. Our findings provide additional insight into the increased susceptibility to malignancies and infections in CKD patients.

## GRAPHICAL ABSTRACT



Clinical  
Kidney  
Journal

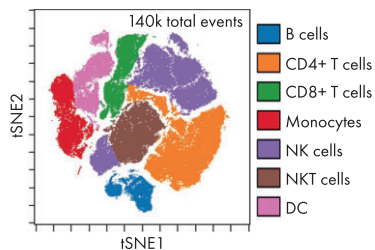
## Deep immune profiling of patients with renal impairment unveils distinct immunotypes associated with disease severity

Chronic kidney disease (CKD) is pathologically correlated with immune dysregulation, but a comprehensive atlas of immune modulation associated with the progression of CKD remains unexplored.

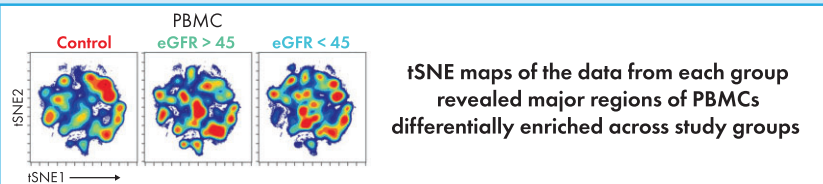
## Methods

Flow cytometry to analyze peripheral blood mononuclear cells (PBMC)

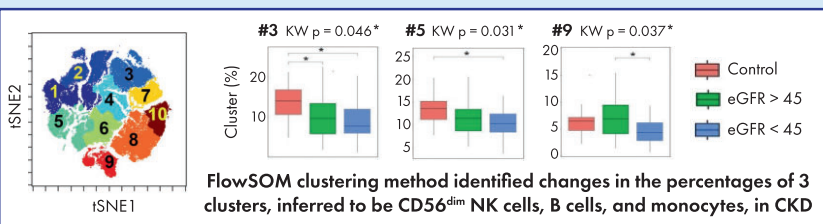
69 with CKD  
19 controls (no CKD)



## Results



tSNE maps of the data from each group revealed major regions of PBMCs differentially enriched across study groups



FlowSOM clustering method identified changes in the percentages of 3 clusters, inferred to be CD56<sup>dim</sup> NK cells, B cells, and monocytes, in CKD

**Conclusion:** Our data-driven approaches identified distinct subsets of monocytes, B cells, and natural killer cells with specific activation status perturbed during renal impairment.

Wu, I.W.  
Clinical Kidney Journal (2022)  
fliawu@yahoo.com  
@CKJsocial

**Keywords:** B lymphocyte, chemokine, chronic kidney disease, cytokine, monocyte, natural killer cell

## INTRODUCTION

Loss of renal function in patients with chronic kidney disease (CKD) causes retention of uremic toxins and cytokines, giving rise to systematic inflammation and immune dysfunction. The uremia-associated defects in the innate and adaptive immune systems have been demonstrated to be interrelated and imperative to recapitulate the prognosis of CKD and to influence its progression into end-stage renal disease (ESRD) [1]. As such, ESRD patients are highly vulnerable to microbial infections [2] and often bear unsatisfactory vaccination responses [3] and an increased susceptibility to malignancies [4], mainly due to accumulation of carcinogenic toxins, alteration in gut microbiota, and a state of acquired immunodeficiency and oxidative stress [5, 6]. In addition, two common comorbidities in CKD, cardiovascular disease [7] and infections [2], both of which have been

largely attributed to dysregulated immunity, together account for up to 70% of death in renal failure, implicating a detrimental role for this ominous disturbance of immune responses in CKD management.

The immune system is mainly composed of cellular and soluble elements, which form a reciprocal interaction against various pathological conditions. It has been noted that diverse cell types of innate and adaptive immune system are affected to a different extent with regard to their numbers and activation status during the progressive loss of kidney function [8]. Specifically, an expansion of proinflammatory CD4<sup>+</sup>CD28<sup>-</sup> T cell [9, 10] and CD14<sup>+</sup>CD16<sup>+</sup> monocyte populations [11, 12] was observed in ESRD patients, whereas a gradual decline in circulating numbers of natural killer (NK) [13, 14] and B cells [15] was associated with the impairment of renal function. Moreover, the number [16]

and function [17] of dendritic cells, one of the most potent professional antigen-presenting cell types in the immune system, were reduced in patients with severe CKD. These uremia-related alterations in immune cell composition might be, to some degree, accounted for by excess generation of oxidative stress and epigenetic modifications, as seen in healthy elderly individuals [1]. Except for changes in cellular components, destruction of kidneys leads to an accumulation of numerous immune-related solutes in the circulation [18–21], as evidenced by the frequent presence of hypercytokinemia and complement activation in renal failure. The combined effects of these immune dysfunctions, conceivably, contribute to multiple complications and are strongly connected to high mortality in CKD.

To date, studies of immune dysregulation in CKD have been mostly focused on a particular immune cell lineage and on the advanced stages of disease [1, 8, 22]. Yet, the dynamic correlation of the immunophenotypes with the disease development in CKD remains to be fully understood. Hence, to test our hypothesis that dysregulated immune responses are associated with renal disease progression, we comprehensively compared peripheral blood mononuclear cells (PBMCs) using high-dimensional flow cytometry and a panel of hematopoiesis- and immune-related solutes, especially for less studied cytokine/chemokine/growth factors, in CKD patients with different disease severities and subjects with normal renal function. Our analyses reveal divergent immune signatures and provide further insights into the shift of immune cell identities and activation status with the progression of kidney failure.

## MATERIALS AND METHODS

### Study cohort

In this study, 19 non-CKD controls and 69 patients (age 20–80 years) with CKD as determined by the K/DOQI Clinical practice guidelines [23] were recruited in the Department of Nephrology at Chang Gung Memorial Hospital, with the approval by the institutional review board. CKD was defined as either the presence of proteinuria or an estimated glomerular filtration rate (eGFR) of  $<60$  mL/min/1.73 m<sup>2</sup> on two separate occasions. All subjects are Taiwanese, and informed consent was obtained from each participant. To explore the disease progression, patients were assigned into two groups, one with an eGFR of  $\geq 45$  mL/min/1.73 m<sup>2</sup> and the other with the values of eGFR  $<45$  mL/min/1.73 m<sup>2</sup>. Since the immune system undergoes dramatic changes related to the age [24], gender [25], and two most common comorbidities in CKD patients—diabetes [26] and hypertension [27]—subjects with normal renal function and matched age, gender, and status of diabetes mellitus and hypertension were enrolled as controls for comparisons and the exclusion of potential confounding factors. Demographic, clinical, anthropometrics and laboratory parameters of participants were assessed at the enrolment. These parameters include blood urea nitrogen, creatinine, potassium, hemoglobin, hematocrit, albumin, calcium, phosphate, Ca-P product, intact parathyroid hormone, high sensitive C-reactive protein, total cholesterol, triglyceride, urine sediments, proteinuria and residual renal creatinine clearance rate. Anthropometric parameters include body weight, body mass index and waist circumference. Cases who neither had been previously treated with immunosuppressants nor had undergone kidney transplant were enrolled in this study. Participants with malignancy, liver cirrhosis, intestinal operation, irritable bowel syndrome, cardiovascular disease (defined as myocardial infarction, documented

Q wave on electrocardiogram, unstable angina, coronary artery disease with stenosis  $>75\%$ , congestive heart failure with an ejection fraction  $<50\%$  and cerebrovascular disease), active infection or pregnancy were excluded from the study. Whole blood (5 mL) was withdrawn for immunotype analysis.

### PBMC collection and staining

At enrollment, PBMCs were isolated from buffy coats using density gradient centrifugation. Blood samples were diluted with phosphate-buffered saline (PBS) (Sigma), layered onto the Ficoll-Hypaque media solution (GE Healthcare), and centrifuged at room temperature for 20 min at 2000 r.p.m. The mononuclear cell layer was carefully removed from the interface and washed twice with PBS. Cells were frozen in CoolCell containers (Corning) in heat-inactivated fetal bovine serum (FBS) (Sigma) supplemented with 10% dimethyl sulfoxide (Sigma) and stored in liquid nitrogen until flow cytometric analysis. For cell staining, frozen human PBMCs were recovered from liquid nitrogen with RPMI1640 with 10% FBS. PBMCs ( $5 \times 10^5$ ) were resuspended in FACS staining buffer (PBS with 1% FBS) and stained with fluorochrome-conjugated antibodies on ice for 20 min. In addition to the KLRG-1-Alexa Fluor® 647 (2388C) that was obtained from R&D Systems, a panel of the following clones of fluorochrome-conjugated antibodies purchased from BD Bioscience was used for cell staining: CD16-BUV496 (3G8), CD19-BUV563 (SJ25C1), IgD-BUV615 (IA6.2), CD4-BUV661 (SK3), CD64-BUV737 (10.1), CD14-BUV805 (M5E2), CD57-BV421 (NK-1), CD3-BV480 (UCHT1), PD-1-BV605 (EH12.1), CD15-BV650 (HI98), CD27-BV711 (M-T271), CD20-BV750 (2H7), CD197-BV786 (2-L1-A), CD45RA-BB515 (HI100), CD94-BB630-P2 (HP-3D9), CD195-BB660-P2 (3A9), CD8-PerCP-Cy5.5 (RPA-TB), CD38-BB790-P (HIT2), CD11c-PE (B-ly6), CD13-PE-CF594 (WM15), CD123-PE-Cy5 (9F5), CD25-PE-Cy7 (2A3), CD56-APC-R700 (NCAM16.2) and HLA-DR-APC-H7 (G46-6). Cells were then washed three times with staining buffer and subjected to flow cytometric analysis.

### Flow cytometry

Data were acquired on a FACSymphony A5.2 (BD Bioscience). Standardized SPHERO rainbow photomultiplier tubes over time and for compensation, Standardized SPHERO rainbow beads (Spherotech) and UltraComp eBeads (ThermoFisher) were used for adjusting photomultiplier tubes over time and for compensation, respectively.

### Data analysis of high-dimensional flow cytometry

viSNE, FlowSOM and CITRUS analyses were conducted on the Cytobank cloud-based platform (Cytobank, Inc.). NK cells and monocytes were analyzed separately. viSNE analysis, a dimensionality reduction method for high-dimensional single-cell data based upon the Barnes–Hut implementation of t-distributed stochastic neighbor embedding (tSNE) [28], was performed using equal sampling of 2000 cells from each FCS file (1200 for NK cells and 450 for monocytes), with all antibody channels, 1000 iterations, a perplexity of 30 and a theta of 0.5. For NK cells, the following markers were used to generate the viSNE maps: KLRG-1, CD56, CD94, CD195, CD38, CD16, CD64, CD57, PD-1, CD15, CD27, CD197, CD11c, CD13 and CD25. For monocytes, the following markers were used: KLRG-1, HLA-DR, CD94, CD195, CD38, CD16, CD64, CD14, PD-1, CD15, CD197, CD11c, CD13, CD123 and CD25. Data concatenation was performed by the FlowJo platform. Resulting viSNE maps were fed into the FlowSOM

clustering algorithm [29]. FlowSOM was conducted with the following parameters: Event Sampling Method: 'Equal'; Desired events per file: '2000' ('1200' for NK cells and '450' for monocytes); Total events actually sampled: '140000' ('84000' for NK cells and '31500' for monocytes); SOM Creation: 'Create a new SOM'; Clustering Method: 'Hierarchical Consensus'; Number metaclusters: '10'; Iterations: '10'. For each cell subset, a new self-organizing map (SOM) was generated using hierarchical consensus clustering on the tSNE axes. For each SOM, 10 metaclusters were identified for comparisons. An additional computational algorithm, CITRUS [30], was used to identify clusters of cell subpopulations that are statistically correlated with the disease severity. CITRUS was performed using the Significance Analysis of Microarrays (SAM) correlative association model (based on a Benjamini-Hochberg corrected  $P$ -value of  $<.01$ ) with the following parameters: Clustering channels: 'select all antibody-conjugate channels'; Compensation: 'File-Internal Compensation'; Association Models: 'Significance Analysis of Microarrays (SAM)—Correlative'; Cluster Characterization: 'Abundance'; Event sampling: 'Equal'; Events sampled per file: '5000'; Minimum cluster size: '1%'; Cross Validation Folds: '5'; False Discovery Rate: '1%'.

### Measurement of cytokines/chemokines/growth factors

Instead of commonly studied proinflammatory cytokines, a panel of 15 hematopoiesis- and immune-related cytokines, chemokines and growth factors pre-selected by the institutional facility were utilized to compare the non-cellular components in the circulation of CKD patients, by using the ProcartaPlex Multiplex Immunoassay Kit (eBioscience) according to the manufacturer's protocol. Each serum sample was tested in duplicate. Plates were read with the Luminex 200 system (Luminex) and analyzed by using ProcartaPlex software (eBioscience).

### Statistical analysis

Differences in clinical indices among groups were determined using Student's  $t$ -test or Kruskal-Wallis test. The levels or proportions of immunotypes were compared by using Wilcoxon rank sum or Kruskal-Wallis test. The connection of immunotype to clinical indices was assessed by Spearman's rank correlation, and the importance was corrected by using the Benjamini-Hochberg procedure. Random Forests [31] models were used to rank each variable independently. For each test, the performance of the model was examined by receiver operating characteristic (ROC) curves using 5-fold cross-validation. Unless otherwise stated, all statistical tests are two-tailed, and a  $P < .05$  is considered statistically significant.

## RESULTS

### Study design and subject characteristics

To explore the association of circulating immunotypes with the progression of CKD, we collected whole blood samples from a cross-sectional cohort of 88 subjects, comprising 69 cases (one group with an eGFR of  $\geq 45$  mL/min/1.73 m<sup>2</sup>,  $n = 44$ ; and the other group with the values of eGFR  $< 45$  mL/min/1.73 m<sup>2</sup>,  $n = 25$ ) and 19 non-CKD controls. To exclude potential confounding factors, non-CKD controls with normal renal function and matched age, gender, and status of diabetes mellitus and hypertension (Table 1) were recruited. The levels of blood urea nitrogen, serum creatinine and eGFR reflect the disease severity among cases.

Cytokine/chemokine/growth factor profiles were collected from all subjects. Among them, PBMCs of 77 participants were subjected to high-dimensional flow cytometry, and 70 samples (14 controls, 35 with eGFR  $\geq 45$  mL/min/1.73 m<sup>2</sup>, and 21 with eGFR  $< 45$  mL/min/1.73 m<sup>2</sup>), passing stringent quality control and file clean-up (e.g. removal of dead cells, debris and doublets), were used for further analyses and comparisons.

### Progressive loss of kidney function results in broad changes in circulating immune cell types and cytokines/chemokines/growth factors

We first compared a panel of cytokine/chemokine/growth factors across groups. The circulating concentrations of stem cell factor (SCF), a cytokine that binds to c-KIT [32], were found to be elevated with the progression of CKD (Fig. 1a and Supplementary data, Fig. S1) and inversely correlated with eGFR (Fig. 1b). This association remained significant after adjusting for hemoglobin levels ( $P = .013$ ), as anemia is a common complication of CKD. In addition, a descending trend in the levels of platelet-derived growth factor BB (PDGF-BB) and brain-derived neurotrophic factor (BDGF) was detected with the disease severity, whereas that of regulated upon activation, normal T cell expressed and presumably secreted (RANTES) and placental growth factor-1 (PlGF-1) were increased in severe CKD (eGFR  $< 45$  mL/min/1.73 m<sup>2</sup>) (Fig. 1a and Supplementary data, Fig. S1).

We next interrogated the populations of PBMCs by using high-dimensional flow cytometry. To obtain more insights, we applied viSNE on the immune cell abundance profiles from all subjects, and the resulting tSNE representation revealed the heterogeneity of major immune cell types (e.g. T, B, NK cells) that can be loosely defined based on marker intensities (Fig. 1c and Supplementary data, Fig. S2). tSNE maps of the data from each group highlighted key regions of PBMCs differentially enriched across study cohorts (Fig. 1d), implying altered abundances of immune cell populations with the disease severities. To further quantify these differences and possibly rule out the subjectivity inherent in manual gating, we performed an unsupervised algorithm, FlowSOM, to cluster the cells (Fig. 1e). This method identified a decrease in the percentages of three clusters ( $P < .05$  by Kruskal-Wallis test), including Clusters 3, 5 and 9 in severe CKD (eGFR  $< 45$  mL/min/1.73 m<sup>2</sup>). Clusters 3 and 9 can be approximately inferred to be CD56<sup>dim</sup> NK cells and B cells, respectively, while Cluster 5 correspond to a combination of CD56<sup>bright</sup> NK cells and a subset of monocytes (Fig. 1c and Supplementary data, Fig. S2). In addition, a positive correlation of eGFR was detected with the abundance of Clusters 5 and 9. These results indicate a global shift of immunotypes during the progression of CKD.

### Progression of CKD is associated with heterogeneous cell subsets and activation of monocytes, NK cells and B cells

To explore the high heterogeneity of peripheral immune cells in detail, we next applied high-dimensional flow cytometric analysis to further investigate the activation and patterns of NK cells (Supplementary data, Fig. S3) in CKD. Among the NK cell populations, there was a decrease in the frequency of CD38<sup>+</sup> cells in severe CKD, as that of PD-1<sup>+</sup> cells was increased in both mild and severe CKD compared with controls (Fig. 2a). Projecting the global NK cells into the tSNE space again revealed major



Table 1: Baseline characteristics of study cohorts.

	All subjects (n = 88)	Control (n = 19)	eGFR		P
			≥45 mL/min/ 1.73 m <sup>2</sup> (n = 44)	eGFR <45 mL/min/ 1.73 m <sup>2</sup> (n = 25)	
Age, years	64.01 ± 5.73	64.26 ± 7.16	63.45 ± 5.14	64.8 ± 5.67	.318
Gender (males), n (%)	43 (48.9)	8 (42.1)	24 (54.5)	11 (44)	.407
Diabetes, n (%)	41 (46.6)	8 (42.1)	21 (47.7)	12 (48)	.983
Hypertension, n (%)	73 (83)	13 (68.4)	38 (86.4)	22 (88)	.849
Gout, n (%)	15 (17)	1 (5.3)	7 (15.9)	7 (28)	.266
Hyperlipidemia, n (%)	33 (37.5)	7 (36.8)	17 (38.6)	9 (36)	.831
Diastolic blood pressure, mmHg	75.16 ± 10.58	74 ± 9.97	75.23 ± 10.13	75.92 ± 12.06	.800
Systolic blood pressure, mmHg	131.49 ± 15.54	127.84 ± 19.05	130 ± 15.06	136.88 ± 12.34	.056
Height, cm	159.36 ± 8.41	159.77 ± 8.97	159.99 ± 7.68	157.94 ± 9.35	.328
Weight, kg	66.37 ± 10.9	61.8 ± 8.62	69.74 ± 11.23	63.89 ± 10.24	.035
Body mass index, kg/m <sup>2</sup>	26.12 ± 3.69	24.22 ± 2.86	27.21 ± 3.85	25.62 ± 3.37	.089
Waist circumference, cm	88.31 ± 10.14	83.28 ± 8.71	91.11 ± 10.34	87.21 ± 9.42	.125
Laboratory parameters					
Blood urea nitrogen, mg/dL	25.15 ± 19.3	13.42 ± 3.58	17.91 ± 5.59	46.8 ± 24.32	<.001*
Serum creatinine, mg/dL	1.66 ± 1.5	0.7 ± 0.14	1.1 ± 0.22	3.37 ± 1.92	<.001*
eGFR, mL/min/1.73 m <sup>2</sup> , CG	58.37 ± 27.85	87.88 ± 21.13	64.51 ± 13.93	25.13 ± 14.85	<.001*
eGFR, mL/min/1.73 m <sup>2</sup> , Epi	59.51 ± 28.63	94.49 ± 8.91	65 ± 13.06	23.25 ± 14.62	<.001*
eGFR, mL/min/1.73 m <sup>2</sup> , MDRD	61.88 ± 45.78	114.24 ± 67.55	61.42 ± 11.52	22.92 ± 13.64	<.001*
Hemoglobin, g/dL	12.73 ± 1.92	13.33 ± 0.87	13.56 ± 1.28	10.82 ± 2.11	<.001*
Serum albumin, g/dL	4.47 ± 0.39	4.52 ± 0.25	4.57 ± 0.28	4.27 ± 0.55	.017
Serum calcium, mg/dL	9.22 ± 0.41	9.25 ± 0.37	9.3 ± 0.33	9.06 ± 0.53	.049
Serum phosphate, mg/dL	3.94 ± 0.75	3.75 ± 0.56	3.76 ± 0.47	4.41 ± 1.05	.007
Serum sodium, mEq/L	140.35 ± 2.14	140.64 ± 1.67	140.12 ± 2.16	140.51 ± 2.44	.505
Serum potassium, mEq/L	4.17 ± 0.45	4.03 ± 0.37	4.09 ± 0.45	4.42 ± 0.42	.005
Carbon dioxide, mmol/L	25.3 ± 3.56	27.37 ± 1.86	25.93 ± 2.18	22.54 ± 4.82	.003*
Uric acid, mg/dL	6.18 ± 1.62	5.39 ± 1.08	6.16 ± 1.31	6.8 ± 2.16	.190
Fasting sugar, mg/dL	119.75 ± 33.69	116.89 ± 21.85	121.32 ± 34.57	119.16 ± 40.04	.815
Glycohemoglobin, %	6.45 ± 1.17	6.38 ± 0.86	6.42 ± 1.11	6.58 ± 1.5	.601
Total cholesterol, mg/dL	186.58 ± 34.71	184.05 ± 25.22	184.64 ± 29.42	191.92 ± 47.94	.495
LDL-cholesterol, mg/dL	104.76 ± 28.44	103.93 ± 26.04	107.14 ± 24.34	101.28 ± 36.47	.479
Triglyceride, mg/dL	152.44 ± 108.89	154.63 ± 100.78	129.75 ± 60.62	190.72 ± 162.2	.081
hs-CRP, mg/L	1.32 (0.55–2.56)	1.04 (0.55–2.13)	1.24 (0.5–2.41)	1.88 (1.21–4.13)	.034
Intact parathyroid hormone, pg/mL	59.9 (36–93.7)	56.6 (29.88–79.58)	56.6 (36.15–80.65)	108.9 (47.1–295.2)	.004*
Vitamin D, ng/mL	27.68 ± 11.12	29.64 ± 11.27	29.71 ± 9.45	22.36 ± 12.46	.010
Urine protein:creatinine ratio, mg/g	138.73 (78.6–514.2)	91.74 (65.8–160.4)	111.89 (61.8–250)	935.93 (202.2–2851)	.002*
Daily urine amount, mL	2005 ± 678.9	1896.4 ± 685.1	2235 ± 654.3	1802.2 ± 649.8	.068

Data are expressed as n (%), mean ± SD or median (1st–3rd quartile).

\*P < .005, compared eGFR ≥45 with eGFR <45 mL/min/1.73 m<sup>2</sup> using Students t-test.

LDL, low-density lipoprotein; hs-CRP, high sensitive C reactive protein; CG, Cockcroft–Gault; Epi, Chronic Kidney Disease Epidemiology Collaboration; MDRD: Modification of Diet in Renal Disease.

differences in densities of particular localized regions across three groups (Fig. 2b and c). In addition, using a FlowSOM clustering approach (Fig. 2d), we found distinct marker expression patterns across different cell clusters (Fig. 2e) and demonstrated a decrease in Cluster 9 (representing cells express KLRG-1, CD38, CD64, CD15 and CD197) in severe CKD compared with controls and mild CKD (P < .05 by Kruskal–Wallis test) (Fig. 2f). The abundance of Cluster 9 was positively correlated with eGFR (Fig. 2g), suggesting that loss of such specific NK population reflects the levels of seriousness in kidney failure.

We next performed deep profiling of monocytes (Supplementary data, Fig. S3) to dissect their patterns in association with renal impairment. Among the monocyte populations, CD38<sup>+</sup> cells were found to be less prevalent in severe CKD than that in either mild CKD or controls (Fig. 3a). Projecting the flow cytometry data for monocytes into tSNE space revealed a global shift of monocyte populations among three cohorts, with separated regions preferentially emerged in

each study group (Fig. 3b and c). In patients with severe CKD, there was a notable decrease in cell densities in tSNE regions enriched for expression of CD38 and PD-1 but negative for CD94 (Fig. 3c). The distribution of CD38 levels in monocytes mirrored the cell densities of particular localized regions across three groups. This observation was supported by further FlowSOM clustering followed by a quantitative analysis. We found that the monocyte immunotype of severe CKD was dominated by the loss of cluster 6 characterized by relatively high expression of KLRG-1, CD38 and PD-1, as compared with monocytes from controls and mild CKD (P < .05 by Kruskal–Wallis test) (Fig. 3d–f). Moreover, a positive correlation between the abundance of Cluster 6 and eGFR was achieved (Fig. 3g), implicating a role for the deprivation of this particular monocyte subset in immune dysregulation of CKD.

For deep profiling of B cell population, our FlowSOM analysis achieved no cluster with statistically significant difference, likely due to a low number of total events seeded. Since

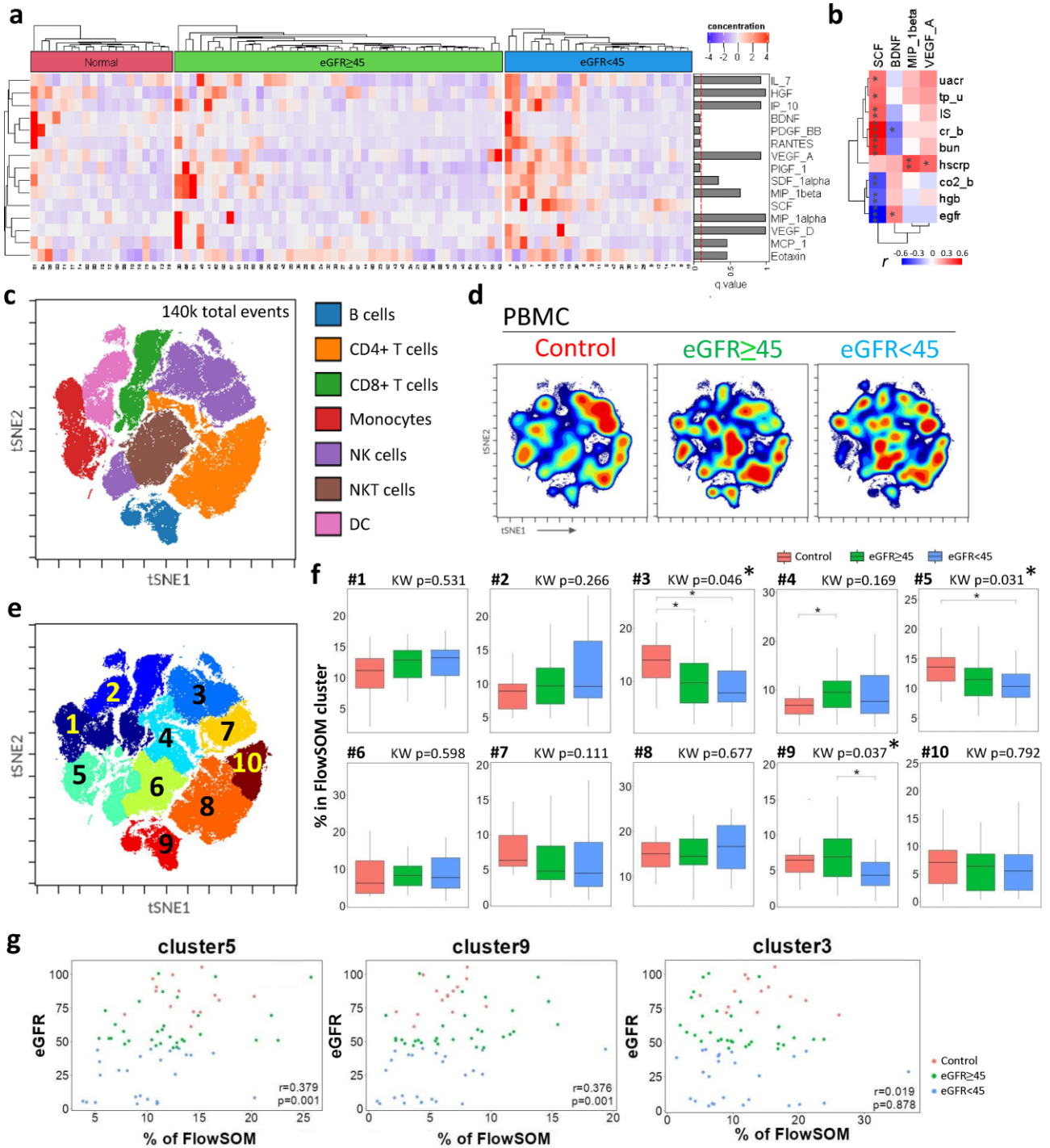


**Figure 1:** Universal characteristics of circulating cytokines/chemokines/growth factors and PBMCs in CKD. (a) Normalized concentrations of cytokines/chemokines/growth factors in CKD group 1 (CKD1; eGFR  $\geq$ 45 mL/min/1.73 m<sup>2</sup>), CKD group 2 (CKD2; eGFR  $<$ 45 mL/min/1.73 m<sup>2</sup>) and non-CKD controls (Control). Red dashed line indicates a q value of 0.1 using Kruskal-Wallis test. (b) Spearman correlation of circulating cytokines/chemokines/growth factors with clinical indices (n = 88, \*q < 0.05, \*\*q < 0.01, \*\*\*q < 0.001). uacr, urine albumin-to-creatinine ratio; tp\_u, total protein in urine; IS, indoxyl sulfate; cr\_b, creatinine in blood; bun, blood urea nitrogen; hscrp, high-sensitivity C-reactive protein; co2-b, CO<sub>2</sub> in blood; hgb, hemoglobin; egfr, estimated filtration glomerular rate. (c, d) Global viSNE projection of PBMCs for all participants pooled and colored by major immune cell lineages loosely defined by marker intensities (c) and PBMCs from the Control, CKD1 and CKD2 groups concatenated and colored according to cell abundance densities (d). NK cells, natural killer cells; DC, dendritic cells; NKT cells, natural killer T cells. (e) viSNE projection of PBMCs identified by FlowSOM clustering. (f) Percentage of PBMCs from each study group in each FlowSOM cluster. The box-plots show the median, the 25th and the 75th percentile in each group. Significance among groups and between groups was determined by Kruskal-Wallis and Wilcoxon rank sum test, respectively. \*P < .05. (g) The correlation of eGFR with the frequencies of cell Clusters 3, 5 and 9, determined by Spearman correlation.

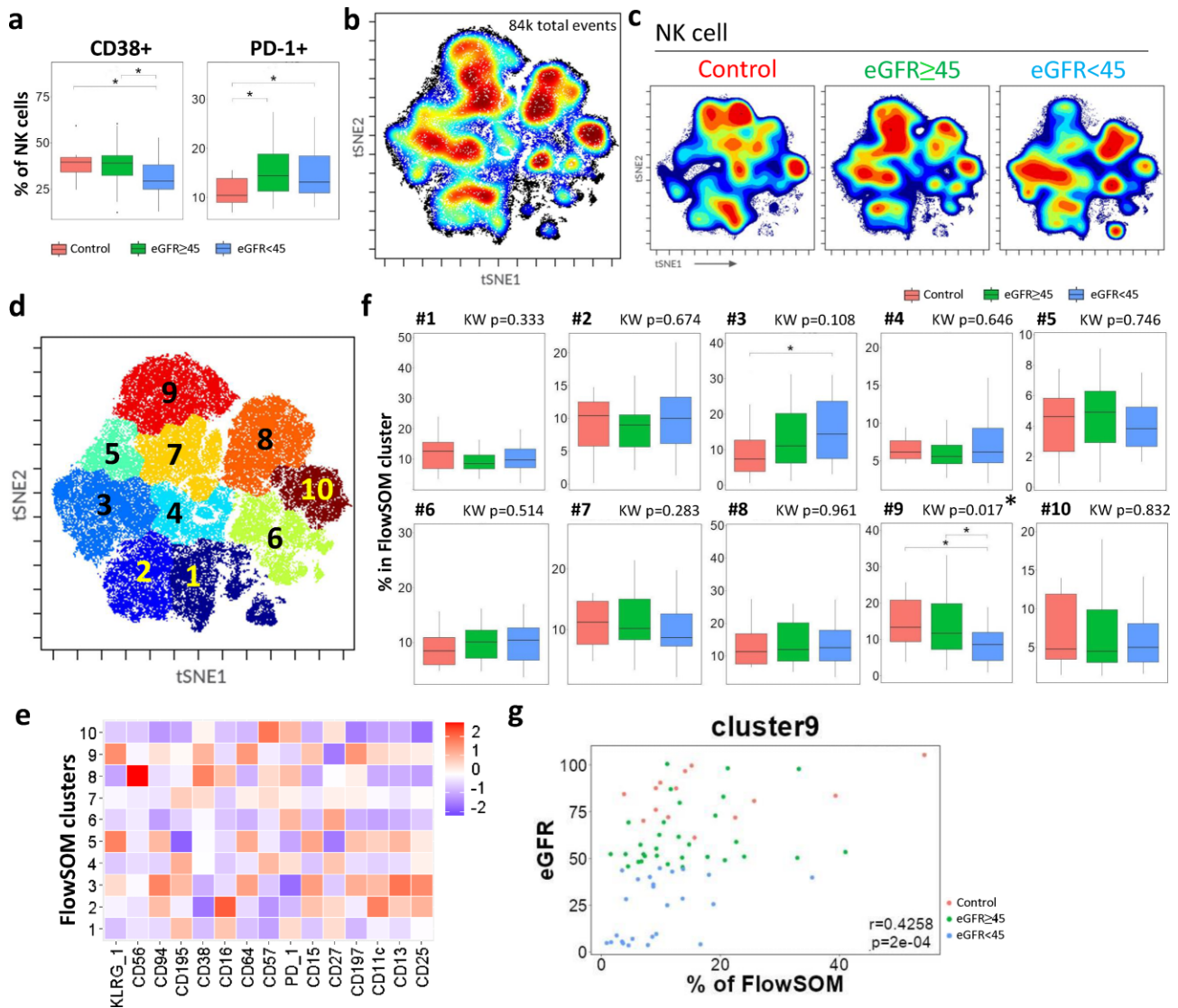


**Figure 2:** Fluctuations in NK cell populations linked to the progression of CKD. (a) Frequencies of PD-1<sup>+</sup> and CD38<sup>+</sup> NK cells. Significance among groups and between groups was determined by Kruskal–Wallis and Wilcoxon rank sum test, respectively. \* $P < .05$ . (b, c) viSNE projection of NK cells for all participants pooled (b) and NK cells from the Control, eGFR  $\geq$ 45 mL/min/1.73 m<sup>2</sup> and eGFR <45 mL/min/1.73 m<sup>2</sup> groups concatenated and colored according to cell abundance densities (c). (d) viSNE projection of NK cells identified by FlowSOM clustering. (e) Mean fluorescence intensity (MFI) of indicated markers across clusters (column-scaled z-scores). (f) Percentage of NK cells from each study group in each FlowSOM cluster. The box-plots show the median, the 25th and the 75th percentile in each group. Significance among groups and between groups was determined by Kruskal–Wallis and Wilcoxon rank sum test, respectively. \* $P < .05$ . (g) The correlation of eGFR with the frequencies of NK cell Cluster 9, determined by Spearman correlation.

progression of CKD, from mild/reversible to severe/irreversible nephron loss, is viewed as a chronic condition [33], we next used CITRUS to compare PBMC profiles from mild and severe CKD patients as a complement to FlowSOM clustering. CITRUS identified four cell clusters that were differentially abundant between cases with eGFR <45 and eGFR  $\geq$ 45 mL/min/1.73 m<sup>2</sup> (Fig. 4a). One significantly altered cluster (279976), highlighted by high expression of CD38, CD94, CD13 and CD123, was descendant cells of the myeloid lineage and representing a monocyte subset (Fig. 4b). Another cluster (279984), enriched for the expression of PD-1, CD197, IgD and HLA-DR, was derived from the lymphoid lineage and defined as a mature B cell population (Fig. 4c). The abundance of both clusters was reduced in severe CKD (eGFR <45 mL/min/1.73 m<sup>2</sup>) (Fig. 4d) and exhibited a positive correlation with eGFR (Fig. 4e). Notably, these results are

compatible with CKD-associated immunotypes identified from the FlowSOM algorithm.

### Immunophenotypic signatures differentiate CKD from non-CKD controls

In order to test the potential of immunotypes to serve as diagnostic markers, we constructed a Random Forests regression model based on 19 cellular and soluble parameters identified in this study (Supplementary data, Table S1) to discriminate cases with from non-CKD controls. Use of 19 immune variables achieved a total area under the ROC curve (AUC) of 0.917 to detect a patient with CKD, with the top-ranking feature being the portion of CD38<sup>+</sup> monocytes (Fig. 5). In addition, a slightly inferior but still satisfactory performance in discriminating mild



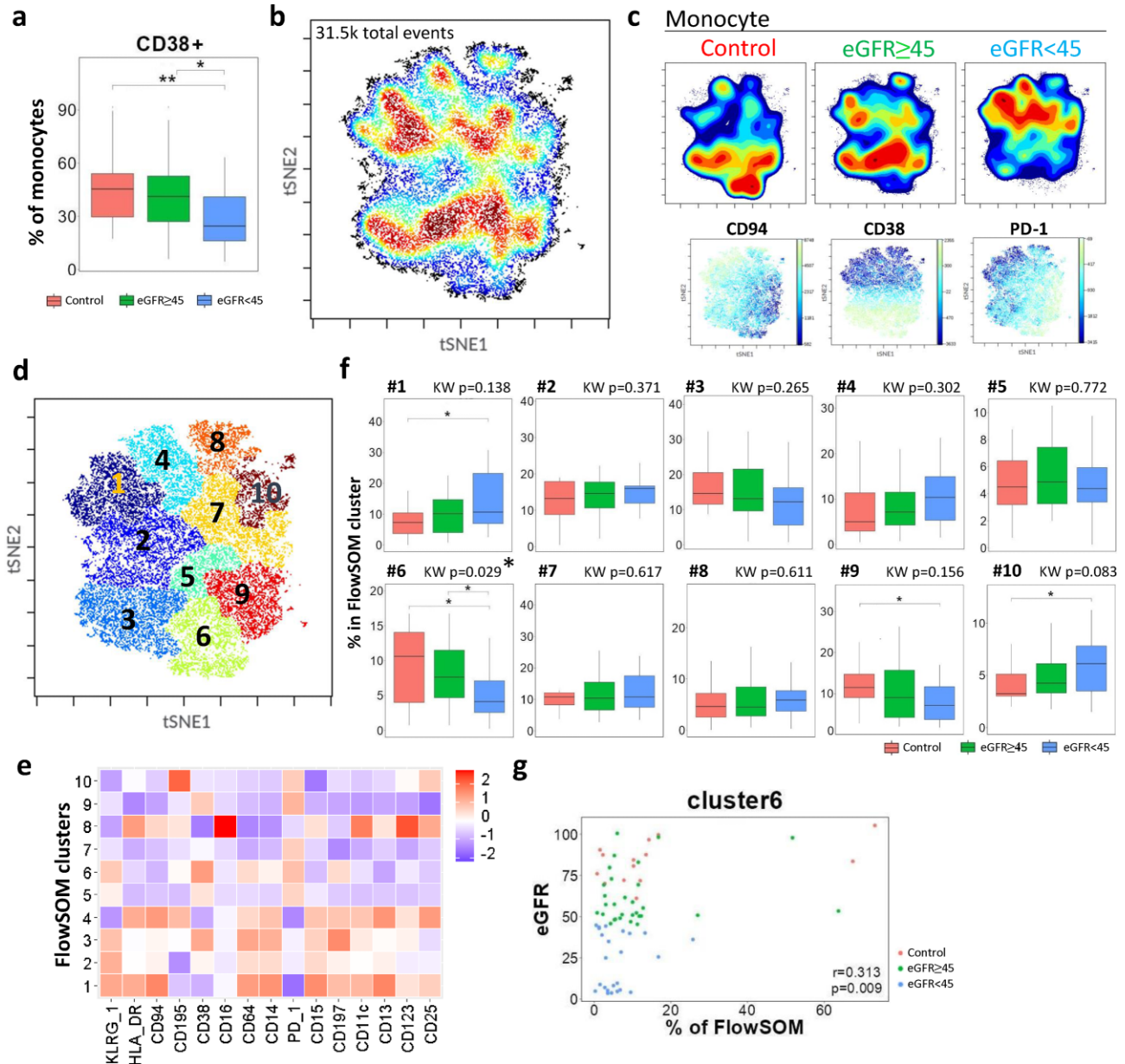


**Figure 3:** Skewing and activation status of monocyte subsets associated with CKD severity. (a) Frequencies of CD38<sup>+</sup> monocytes. Significance among groups and between groups was determined by Kruskal–Wallis and Wilcoxon rank sum test, respectively. \* $P < .05$ ; \*\* $P < .01$ . (b) viSNE projection of monocytes for all participants pooled. (c) viSNE maps for monocytes from the Control, eGFR  $\geq$ 45 mL/min/1.73 m<sup>2</sup> and eGFR  $<$ 45 mL/min/1.73 m<sup>2</sup> groups concatenated and colored according to cell abundance densities (top) and from all participants pooled and colored by the expression of indicated markers (bottom). (d) viSNE projection of monocytes identified by FlowSOM clustering. (e) MFI of indicated markers across clusters (column-scaled z-scores). (f) Percentage of monocytes from each study group in each FlowSOM cluster. The box-plots show the median, the 25th and the 75th percentile in each group. Significance among groups and between groups was determined by Kruskal–Wallis and Wilcoxon rank sum test, respectively. \* $P < .05$ . (g) The correlation of eGFR with the frequencies of monocyte Cluster 6 determined by Spearman correlation.

CKD from the controls, with an AUC of 0.889, was obtained. Our results reveal promising avenues for early diagnosis of CKD via specific immunotypes.

## DISCUSSION

Progressive loss of kidney function causes a highly dynamic skewing of immune modulation. Changes in the immune system predispose patients to develop infections which in turn lead to an increased risk of inflammatory, cardiovascular diseases and many comorbidities. As renal disease often manifests

clinically only when substantial damage has already occurred, new diagnostic and therapeutic strategies must be developed to halt further progression and even trigger appropriate tissue recovery. With a growing number of simultaneously measurable parameters, current advances in flow cytometry have permitted the exhibition of phenotypic heterogeneity of leukocytes and identification of rare and well-characterized cell subsets with novel behaviors. In the present study, we conducted deep profiling of PBMCs by using high-dimensional flow cytometry and circulating cytokines/chemokines/growth factors in CKD patients with different disease severities and subjects with



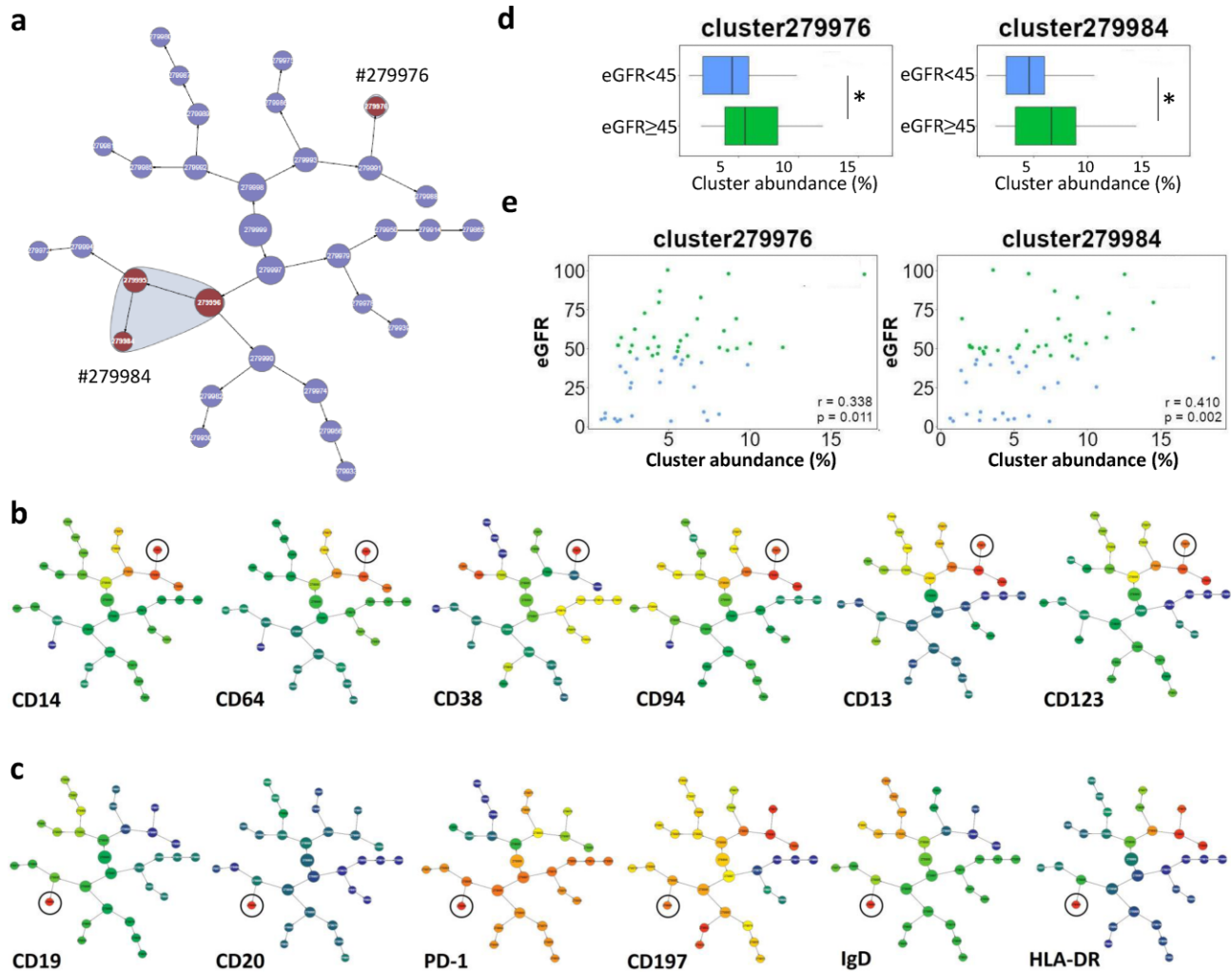


**Figure 4:** Identification of differentially abundant immune cell subsets between mild and advanced CKD patients. (a) A radial hierarchical tree of cell subsets was produced by the CITRUS algorithm. Each node denotes a subset of cells, and each edge points from a parent node to its daughter node(s). Cell subsets of statistically significant differential abundance between CKD group 1 (eGFR  $\geq 45$  mL/min/1.73 m<sup>2</sup>) and CKD group 2 (eGFR  $< 45$  mL/min/1.73 m<sup>2</sup>) are highlighted in dark red. (b, c) The nodes circled in black indicate high or positive expression of a surface marker. Expression profiling demonstrates that cluster 279984 and 279976 correspond to PD-1<sup>+</sup>CD197<sup>+</sup>IgD<sup>+</sup>HLA-DR<sup>+</sup> mature B cells (b) and CD38<sup>+</sup>CD94<sup>+</sup>CD13<sup>+</sup>CD123<sup>+</sup> monocytes (c), respectively. (d) Abundances of Cluster 279984 and 279976 in eGFR  $\geq 45$  mL/min/1.73 m<sup>2</sup> and eGFR  $< 45$  mL/min/1.73 m<sup>2</sup>. \*Benjamini-Hochberg corrected P-value of  $< .01$  using the Significance Analysis of Microarrays correlative association model. (e) The correlation of eGFR with the frequencies of CITRUS clusters, determined by Spearman correlation.

normal renal function. To avoid the subjectivity inherent in manual gating [34], we utilized data-driven approaches to identify immunological signatures dysregulated during renal impairment. Our findings, to some extent, account for the increased susceptibility to malignancies and infections in CKD patients.

NK cells represent a pivotal player of innate immune system and exert a prompt immunological reaction modulated by the presence of activating and inhibiting receptors. Levels of activation markers, CD69 and NKP44, were found to be elevated in NK cells from ESRD patients [14], whereas reduced expression of an activating receptor, NKG2D, was observed in NK cells from patients receiving dialysis [13]. Here, our unsupervised clustering method demonstrated a loss of an NK subset (Cluster 9) expressing KLRG-1, CD38, CD64, CD15 and CD197 in severe CKD. Among these surface proteins, CD38 is an activation marker that triggers cytotoxic responses in human NK cells [35]. CD197, also known as C-C chemokine receptor type 7 (CCR7), plays a key role in induction of NK cell migration toward lymph nodes [36], as

CD64 mainly contributes to a vital effector function of NK cells, the antibody-dependent cell-mediated cytotoxicity [37]. The decreased portion of this activated NK cell subset and their possible reduced function might result in impaired tumor immune surveillance and augmented vulnerability to microbial infections in patients with ESRD as a result of decreased killing of stressed cells. In addition to a reduction of CD38<sup>+</sup> NK cells in severe CKD, we noted that PD-1<sup>+</sup> NK cells were more prevalent in CKD patients. Unlike T cells, NK cells present in the peripheral blood of healthy individuals do not express PD-1 on their surface [38], and PD-1 expression on NK cells was linked to intra-tumoral NK cell dysfunction, indicating a weaker anti-cancer function in PD-1<sup>+</sup> NK cells [39, 40]. Our findings provide extra immunological clues about multiple complications and resulting high mortality in CKD.

Different from NK cells as the lymphoid lineage cells, monocytes are derived from the bone marrow and circulate in the blood before further differentiating into macrophages or

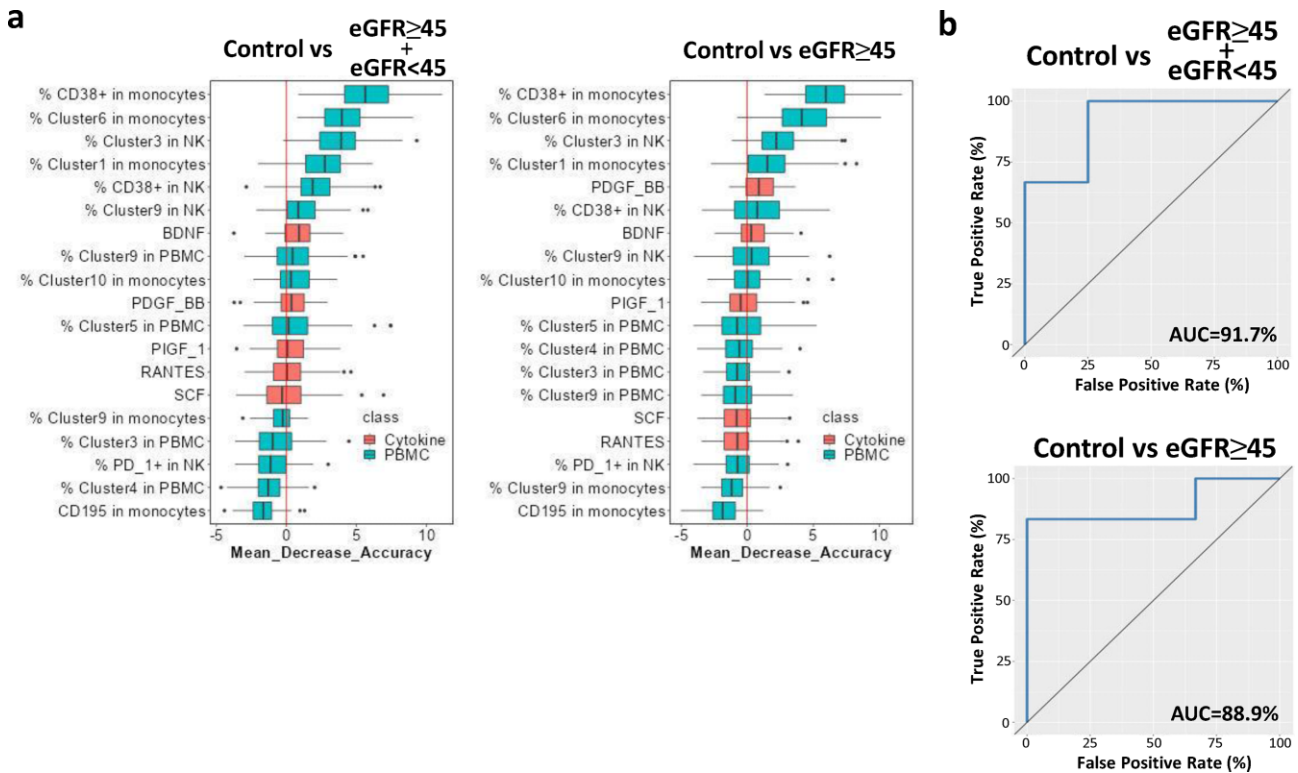


**Figure 5:** Performance of distinguishing CKD cases from the controls. (a) Immunophenotypic markers for detecting patients with CKD (eGFR  $\geq$ 45 + eGFR  $<$ 45 mL/min/1.73 m $^2$ ,  $n = 56$ ) and mild CKD (eGFR  $\geq$ 45 mL/min/1.73 m $^2$ ,  $n = 35$ ) from the controls ( $n = 14$ ) identified from Random Forests classifiers. Markers are ranked in descending order of their importance to the accuracy of the model. The boxes represent 25th–75th percentiles, and black lines indicate the median. (b) ROC curves depict the trade-off between true and false positive rates for detecting patients with CKD and mild CKD. AUC, the total area under the ROC curve.

dendritic cells. Patients with ESRD often bear an expansion of a proinflammatory CD14 $^{++}$ CD16 $^{+}$  monocyte population [11, 12], which is known to confer a future risk of an atherosclerotic event. Consistently, an increase in one similar CD14 $^{++}$ CD16 $^{+}$  monocyte subset (Cluster 1), enriched for the expression of CD94, CD15 and CD13, was also observed in our severe CKD cases. Moreover, we identified a decline in a distinct monocyte subset (Cluster 6), highlighted by high expression of CD38 and PD-1, in advanced stages of the disease. CD38 can establish lateral associations with class II major histocompatibility complex (MHC) in monocytes [41], enabling an efficient presentation of cancer neoantigens or foreign antigens from pathogens. In addition to co-receptor functions, CD38, through its intrinsic enzymatic activities, can also use nicotinamide adenine dinucleotide (NAD) as a substrate to generate second messengers, such as cyclic-ADP ribose (cADPR) [42]. A protective role of CD38 NADase activities against pathogens has been proposed, as pharmaceutical depletion of cellular NAD levels in human monocytes was shown to attenuate TLR4-mediated inflammatory responses to LPS [43]. Taken together, the increase of a proinflammatory CD14 $^{++}$ CD16 $^{+}$  monocyte population (Cluster 1) and loss of one particular monocyte subset (Cluster 6) in severe CKD, as well as the observation that distribution of CD38 levels in monocytes reflected the severity of renal impairment in the present study, in part, account for common comorbidities in CKD, including cardiovascular diseases, infections and cancers.

B lymphocytes are central to the adaptive humoral immune system and mainly responsible for the generation of antigen-specific immunoglobulin targeting invasive pathogens.

In patients with ESRD, reduced numbers of naïve and memory B cells have been reported [15]. Here, a decline in the frequency of a mature B cell cluster, with high expression levels of CD19, CD20, PD-1, CD197, IgD and HLA-DR, was detected in severe CKD compared with mild CKD. A tumor-infiltrating PD-1 $^{\text{high}}$  B cell subset, exhibiting a unique CD5 $^{\text{high}}$ CD27 $^{\text{high}}$ CD38 $^{\text{dim}}$  phenotype that differs from conventional regulatory B cells, was found to suppress tumor-specific T cell responses in liver cancer [44]. Intriguingly, one recent large population cohort study of cancer risk in CKD patients indicates that overall cancer risk was increased in mild to moderate CKD and among transplant recipients, but not in advanced kidney disease [45]. Except for not taking many potential severity-specific confounders into consideration, this discrepancy may be accounted for by further stratification analyses for site-specific cancer incidence, since breast, colon and prostate cancer were less frequent in advanced CKD, and the risk for multiple myeloma, kidney cancer and bladder tumor was particularly increased in CKD. Moreover, it is unclear whether PD-1 $^{+}$  peripheral B cells also possess immunosuppressive activities against pathogens or tumor cells. In addition to PD-1 with uncertain B cell functions, IgD, belonging to an ancient form of immune surveillance strategically positioned at the sites of antigen entry, is known to be present in mature B cells [46], as HLA-DR is a class II MHC molecule responsible for antigen presentation to T cells. In concordance with B cell lymphopenia frequently seen in ESRD patients, we observed a decreased abundance of a mature B cell subset in severe CKD. Yet, whether the loss of such B cell population affects the generation of antigen-specific immunoglobulins and subsequently leads to attenuated

serological responses to vaccines in uremic conditions requires further investigations.

Despite novel insights into the ability to connect immune signatures to CKD severity provided here, additional work is needed to address several limitations of the present study. One issue is that the size of our study cohort is relatively small for deep immune profiling of CKD patients. Considering successful identification of cell subsets consistent with the existing literature and accounting for common comorbidities in CKD, we acknowledge that many more CKD-associated immunotypes are presumably to be found in a larger sample size. Another limitation is the multiple testing burden derived from the high dimensionality of our data. Even though we decreased the number of tests by using FlowSOM clustering, the difference was marginal as considering multiple testing. Moreover, binary comparisons (e.g. one immune subset versus one clinical feature) may fail to completely extract the meaning of high-dimensional dataset. Taken together, our study provides a compendium of immunophenotypic data and identifies specific immune cell identities and activation status associated with the progression of kidney failure.

## SUPPLEMENTARY DATA

Supplementary data are available at [ckj](#) online.

## ACKNOWLEDGEMENTS

The authors are grateful to the Tissue Bank at Chang Gung Memorial Hospital, Keelung for sample preparation and to the Advanced Immunology Laboratory at Chang Gung Memorial Hospital for the technical support of high-dimensional flow cytometry services. This study was supported by research grants from the Ministry of Science and Technology, Taiwan (MOST-109-2320-B-182A-017, MOST-110-2320-B-182A-012-MY3, MOST-110-2314-B-182A-053-MY3) and from the Chang Gung Memorial Hospital (BMRPE97, CMRPG2J024, CRRPG2H0124, CORPG3K0251, CMRPG2M0201 and CMRPG2C0342).

## AUTHORS' CONTRIBUTIONS

I-W.W., W.-P.H. and S.-C.S. performed conceptualization. I-W.W., H.-Y.Y. and C.-K.H. prepared sampling. I-W.W., Y.-L.W., L.-C.C. and Y.-L.C. performed data analysis. Y.-C.T. and W.-H.C. performed data curation. I-W.W. and S.-C.S. performed writing. C.-W.Y., W.-P.H. and S.-C.S. performed supervision.

## DATA AVAILABILITY STATEMENT

The datasets generated during and/or analyzed during the current study are available from the corresponding author on reasonable request, in accordance with the institutional data sharing policy.

## CONFLICT OF INTEREST STATEMENT

All the authors declared no competing interests.

## REFERENCES

- Betjes MG. Immune cell dysfunction and inflammation in end-stage renal disease. *Nat Rev Nephrol* 2013;9:255–65. <https://doi.org/10.1038/nrneph.2013.44>
- Sarnak MJ, Jaber BL. Mortality caused by sepsis in patients with end-stage renal disease compared with the general population. *Kidney Int* 2000;58:1758–64. <https://doi.org/10.1111/j.1523-1755.2000.00337.x>
- Verkade MA, van de Wetering J, Klepper M. et al. Peripheral blood dendritic cells and GM-CSF as an adjuvant for hepatitis B vaccination in hemodialysis patients. *Kidney Int* 2004;66:614–21. <https://doi.org/10.1111/j.1523-1755.2004.00781.x>
- Stewart JH, Vajdic CM, van Leeuwen MT. et al. The pattern of excess cancer in dialysis and transplantation. *Nephrol Dial Transplant* 2009;24:3225–31. <https://doi.org/10.1093/ndt/gfp331>
- Hu M, Wang Q, Liu B. et al. Chronic kidney disease and cancer: inter-relationships and mechanisms. *Front Cell Dev Biol* 2022;10:868715. <https://doi.org/10.3389/fcell.2022.868715>
- Vanholder R, Ringoir S. Infectious morbidity and defects of phagocytic function in end-stage renal disease: a review. *J Am Soc Nephrol* 1993;3:1541–54. <https://doi.org/10.1681/ASN.V391541>
- Foley RN, Parfrey PS, Sarnak MJ. Clinical epidemiology of cardiovascular disease in chronic renal disease. *Am J Kidney Dis* 1998;32:S112–9. <https://doi.org/10.1053/ajkd.1998.v32.pm9820470>
- Cohen G. Immune dysfunction in uremia 2020. *Toxins (Basel)* 2020;12:439. <https://doi.org/10.3390/toxins12070439>
- Betjes MG, Huisman M, Weimar W. et al. Expansion of cytolytic CD4+CD28- T cells in end-stage renal disease. *Kidney Int* 2008;74:760–7. <https://doi.org/10.1038/ki.2008.301>
- Yadav AK, Jha V. CD4+CD28null cells are expanded and exhibit a cytolytic profile in end-stage renal disease patients on peritoneal dialysis. *Nephrol Dial Transplant* 2011;26:1689–94. <https://doi.org/10.1093/ndt/gfr010>
- Scherberich JE, Estner H, Segerer W. Impact of different immunosuppressive regimens on antigen-presenting blood cells in kidney transplant patients. *Kidney Blood Press Res* 2004;27:177–80. <https://doi.org/10.1159/000079807>
- Heine GH, Ulrich C, Seibert E. et al. CD14(++)CD16+ monocytes but not total monocyte numbers predict cardiovascular events in dialysis patients. *Kidney Int* 2008;73:622–9. <https://doi.org/10.1038/sj.ki.5002744>
- Peraldi MN, Berrou J, Dulphy N. et al. Oxidative stress mediates a reduced expression of the activating receptor NKG2D in NK cells from end-stage renal disease patients. *J Immunol* 2009;182:1696–705. <https://doi.org/10.4049/jimmunol.182.3.1696>
- Vacher-Coponat H, Brunet C, Lyonnet L. et al. Natural killer cell alterations correlate with loss of renal function and dialysis duration in uraemic patients. *Nephrol Dial Transplant* 2008;23:1406–14. <https://doi.org/10.1093/ndt/gfm596>
- Descamps-Latscha B, Chatenoud L. T cells and B cells in chronic renal failure. *Semin Nephrol* 1996;16:183–91.
- Hesselink DA, Betjes MG, Verkade MA. et al. The effects of chronic kidney disease and renal replacement therapy on circulating dendritic cells. *Nephrol Dial Transplant* 2005;20:1868–73. <https://doi.org/10.1093/ndt/gfh897>
- Verkade MA, van Druningen CJ, Vaessen LM. et al. Functional impairment of monocyte-derived dendritic cells in patients with severe chronic kidney disease. *Nephrol Dial Transplant* 2007;22:128–38. <https://doi.org/10.1093/ndt/gfl519>
- Pascual M, Steiger G, Estreicher J. et al. Metabolism of complement factor D in renal failure. *Kidney Int* 1988;34:529–36. <https://doi.org/10.1038/ki.1988.214>
- Pereira BJ, Shapiro L, King AJ. et al. Plasma levels of IL-1 beta, TNF alpha and their specific inhibitors in undialyzed chronic renal failure, CAPD and hemodialysis patients. *Kidney Int* 1994;45:890–6. <https://doi.org/10.1038/ki.1994.117>

20. Kaizu Y, Kimura M, Yoneyama T et al. Interleukin-6 may mediate malnutrition in chronic hemodialysis patients. *Am J Kidney Dis* 1998;31:93–100. <https://doi.org/10.1053/ajkd.1998.v31.pm9428458>
21. Descamps-Latscha B, Herbelin A, Nguyen AT et al. Balance between IL-1 beta, TNF-alpha, and their specific inhibitors in chronic renal failure and maintenance dialysis. Relationships with activation markers of T cells, B cells, and monocytes. *J Immunol* 1995;154:882–92.
22. Kato S, Chmielewski M, Honda H et al. Aspects of immune dysfunction in end-stage renal disease. *Clin J Am Soc Nephrol* 2008;3:1526–33. <https://doi.org/10.2215/CJN.00950208>
23. National Kidney Foundation. K/DOQI clinical practice guidelines for chronic kidney disease: evaluation, classification and stratification. *Am J Kidney Dis* 2002;39:S1–266.
24. Weyand CM, Goronzy JJ. Aging of the immune system. Mechanisms and therapeutic targets. *Ann Am Thorac Soc* 2016;13 Suppl 5:S422–8. <https://doi.org/10.1513/AnnalsATS.201602-095AW>
25. Klein SL, Flanagan KL. Sex differences in immune responses. *Nat Rev Immunol* 2016;16:626–38. <https://doi.org/10.1038/nri.2016.90>
26. Geerlings SE, Hoepelman AI. Immune dysfunction in patients with diabetes mellitus (DM). *FEMS Immunol Med Microbiol* 1999;26:259–65. <https://doi.org/10.1111/j.1574-695X.1999.tb01397.x>
27. Fernandez-Ruiz I. Immune system and cardiovascular disease. *Nat Rev Cardiol* 2016;13:503. <https://doi.org/10.1038/nrcardio.2016.127>
28. Amir el AD, Davis KL, Tadmor MD et al. viSNE enables visualization of high dimensional single-cell data and reveals phenotypic heterogeneity of leukemia. *Nat Biotechnol* 2013;31:545–52. <https://doi.org/10.1038/nbt.2594>
29. Van Gassen S, Callebaut B, Van Helden MJ et al. FlowSOM: using self-organizing maps for visualization and interpretation of cytometry data. *Cytometry A* 2015;87:636–45. <https://doi.org/10.1002/cyto.a.22625>
30. Bruggner RV, Bodenmiller B, Dill DL et al. Automated identification of stratifying signatures in cellular subpopulations. *Proc Natl Acad Sci USA* 2014;111:E2770–7. <https://doi.org/10.1073/pnas.1408792111>
31. Breiman L. Random forests. *Machine Learning* 2001;45:5–32. <https://doi.org/10.1023/A:1010933404324>
32. Ashman LK. The biology of stem cell factor and its receptor C-kit. *Int J Biochem Cell Biol* 1999;31:1037–51. [https://doi.org/10.1016/S1357-2725\(99\)00076-X](https://doi.org/10.1016/S1357-2725(99)00076-X)
33. Levey AS, de Jong PE, Coresh J et al. The definition, classification, and prognosis of chronic kidney disease: a KDIGO controversies conference report. *Kidney Int* 2011;80:17–28. <https://doi.org/10.1038/ki.2010.483>
34. Maecker HT, Rinfret A, D'Souza P et al. Standardization of cytokine flow cytometry assays. *BMC Immunol* 2005;6:13. <https://doi.org/10.1186/1471-2172-6-13>
35. Sconocchia G, Titus JA, Mazzoni A et al. CD38 triggers cytotoxic responses in activated human natural killer cells. *Blood* 1999;94:3864–71. <https://doi.org/10.1182/blood.V94.11.3864>
36. Marcenaro E, Cantoni C, Pesce S et al. Uptake of CCR7 and acquisition of migratory properties by human KIR+ NK cells interacting with monocyte-derived DC or EBV cell lines: regulation by KIR/HLA-class I interaction. *Blood* 2009;114:4108–16. <https://doi.org/10.1182/blood-2009-05-222265>
37. Snyder KM, Hullsiek R, Mishra HK et al. Expression of a recombinant high affinity IgG Fc receptor by engineered NK cells as a docking platform for therapeutic mAbs to target cancer cells. *Front Immunol* 2018;9:2873.
38. Pesce S, Greppi M, Tabellini G et al. Identification of a subset of human natural killer cells expressing high levels of programmed death 1: a phenotypic and functional characterization. *J Allergy Clin Immunol* 2017;139:335–46. e3. <https://doi.org/10.1016/j.jaci.2016.04.025>
39. Liu Y, Cheng Y, Xu Y et al. Increased expression of programmed cell death protein 1 on NK cells inhibits NK-cell-mediated anti-tumor function and indicates poor prognosis in digestive cancers. *Oncogene* 2017;36:6143–53. <https://doi.org/10.1038/onc.2017.209>
40. Trefny MP, Kaiser M, Stanczak MA et al. PD-1(+) natural killer cells in human non-small cell lung cancer can be activated by PD-1/PD-L1 blockade. *Cancer Immunol Immunother* 2020;69:1505–17. <https://doi.org/10.1007/s00262-020-02558-z>
41. Zilber MT, Setterblad N, Vasselon T et al. MHC class II/CD38/CD9: a lipid-raft-dependent signaling complex in human monocytes. *Blood* 2005;106:3074–81. <https://doi.org/10.1182/blood-2004-10-4094>
42. Chini EN. CD38 as a regulator of cellular NAD: a novel potential pharmacological target for metabolic conditions. *Curr Pharm Des* 2009;15:57–63. <https://doi.org/10.2174/138161209787185788>
43. Yang K, Lauritzen KH, Olsen MB et al. Low cellular NAD(+) compromises lipopolysaccharide-induced inflammatory responses via inhibiting TLR4 signal transduction in human monocytes. *J Immunol* 2019;203:1598–608. <https://doi.org/10.4049/jimmunol.1801382>
44. Xiao X, Lao XM, Chen MM et al. PD-1hi identifies a novel regulatory B-cell population in human hepatoma that promotes disease progression. *Cancer Discov* 2016;6:546–59. <https://doi.org/10.1158/2159-8290.CD-15-1408>
45. Kitchlu A, Reid J, Jeyakumar N et al. Cancer risk and mortality in patients with kidney disease: a population-based cohort study. *Am J Kidney Dis* 2022; <https://doi.org/10.1053/ajkd.2022.02.020>
46. Gutzeit C, Chen K, Cerutti A. The enigmatic function of IgD: some answers at last. *Eur J Immunol* 2018;48:1101–13. <https://doi.org/10.1002/eji.201646547>